J. Plasma Physics (2001), *vol.* 65, *part* 1, *pp.* 1–28. Printed in the United Kingdom

Viscous interface instability supporting free-surface currents in a hydromagnetic rotating fluid column

YUSRY O. EL-DIB

Department of Mathematics, Faculty of Education, Ain Shams University, Helioplis, Cairo, Egypt

(Received 5 October 1998 and in revised form 22 September 1999)

Abstract. The stabilization of a viscous interface stressed by an oscillating magnetic field is investigated. Account is taken of the influence of free-surface currents on the effective solidly rotating fluid column. Only azimuthal modes are considered in the linear perturbation. The dispersion relation with or without free-surface currents is obtained in the form of a linear Mathieu equation with complex coefficients. It is found that there is a nonlinear relation between the surface current density and both the stratified viscosity and the stratified azimuthal magnetic field. The surface currents disappear on the interface of the fluid column when the stratified magnetic field has the value of unity. At this value, a coupled parametric resonance occurs in the absence of angular velocity. The magnetic field plays a stabilizing role. This role increases with increasing surface currents. The angular velocity plays a destabilizing role, while the field frequency plays a stabilizing role and acts against the angular velocity. The stratified viscosity plays a damping role in the presence of the surface current density, while, in the absence of a surface current, it plays two opposite roles corresponding to the presence or absence of the field frequency. A set of graphs are used to illustrate the relation between the presence of free-surface currents and both the viscosity and the azimuthal magnetic field.

1. Introduction

The investigation of the capillary instability of an infinitely long rotating cylindrical fluid column has classical origins dating back to the time of Lord Rayleigh (1878). This subject has been carefully and continuously studied ever since jet propulsion became technologically feasible. More recently, the floating-zone technique of crystal growth, described for example by Schwabe (1988), has led to renewed interest in problems of this type.

The stability of a rigidly rotating fluid column was studied by Alterman (1961). It was found that, under certain conditions, the rotation may have a stabilizing or a destabilizing effect. Hocking and Michael (1959) demonstrated that rotation has a destabilizing effect. Bauer (1983, 1984, 1989) analysed a rigidly rotating fluid column in a variety of geometries.

The effect of a uniform axial magnetic field upon the capillary instability of a non-rotating fluid column was addressed by Chandrasekhar (1961). Nayyar and Trehan (1963) generalized Chandrasekhar's method, and gave the corresponding analysis for non-axisymmetric perturbations, which they found

always to be stable, just as they are when the magnetic field is absent. Srivistava and Kushwaha (1967) investigated the effect of an axial magnetic field on the capillary instability of a non-rotating column of perfectly conducting viscous fluid. Gupta (1964) investigated the capillary instability of a non-rotating fluid column carrying an axial current both with and without an axial magnetic field. Verma and Verma (1965) considered the capillary instability of a rotating fluid column carrying an axial current in a twisted magnetic field. Terhan et al. (1965) generalized the earlier work of Nayyar and Terhan (1963) to investigate the effect of including the Hall current. Wilson (1992) extended the method used by Gillis and Kaufman (1961) for a rigidly rotating column of viscous fluid to include the presence of a uniform axial magnetic field.

The phenomena of parametric resonance arises in many branches of physics and engineering. Donnelly (1969) found experimentally that cylindrical Couette flow can be stabilized somewhat by having the velocity of the inner wall oscillate about a mean value. The stability of a liquid jet under a time-dependent electric field was investigated by Mohamed and Nayyar (1970) and Mohamed et al. (1985). More recently, El-Dib (1996) carried out a stability analysis of an oscillating liquid column subjected to periodic rigid-body rotation. A Mathieu equation with a parametric imaginary damping term was obtained and analyzed. El-Dib and Moatimid (1994) and Moatimid and El-Dib (1994) developed a theoretical analysis to investigate the effect of periodic rotation of a cylindrical liquid jet under the influence of an axially and radially constant electric field.

In the present work, we extend the method used by El-Dib (1997) for a rigidly rotating column of a weakly viscous fluid to include the presence of a surface current density on the fluid interface. The fluid column is held by capillary forces in the presence of an azimuthal periodic magnetic field. We are concerned with the influence of surface currents on the stability of non-axisymmetric disturbances. The main objective of this study is to illustrate the relation between the presence of the surface current density and both the fluid viscosity and the azimuthal magnetic field.

The paper is organized as follows. In the first part, we formulate the model developed in the absence of free-surface currents. The relation between the surface current density and the azimuthal magnetic field is illustrated numerically in the second part. The basic equations governing the flow are presented in Sec. 2. The boundary conditions used in the hydromagnetic field model are described in Sec. 3. The linearized equations are highlighted in Sec. 4. Section 5 is devoted to the study of the case where there are no surface currents at the surface of separation. The effect of an interface with a surface current density is examined in Sec. 6. Numerical estimations and conclusions are illustrated in Secs 5.2, 6.1 and 6.3.

2. Problem statement and basic equations

We consider the motion of a homogeneous magnetized fluid column of infinite extent. The column is assumed to have a viscous interface. In its equilibrium configuration, the interfacial surface is a circular cylinder of radius R. The column performs a rigid-body rotation, in a weightless condition, with a

https://doi.org/10.1017/S0022377801001003 Published online by Cambridge University Press

constant angular velocity Ω_1 about its axis of symmetry. The fluid of the column has density ρ_1 and magnetic permeability μ_1. The column is embedded in a rotating unbounded fluid having density ρ_2, magnetic permeability μ_2 and a constant angular velocity Ω_2. The fluids are homogeneous, incompressible and non-conducting, and exhibit interfacial tension. The tension forces act as restoring forces to the otherwise damped oscillations of the interfacial surfaces.

The system is subjected to an azimuthal periodic magnetic field with a forcing frequency $\tilde{\omega}$:

$$\mathbf{H} = H_j \cos\tilde{\omega}t\,\mathbf{e}_\theta, \qquad j = 1, 2, \tag{2.1}$$

where $\mathbf{e}_\theta$ is the unit vector in the θ direction. In the equilibrium configuration, we shall be concerned with two cases:

(A) there are no free-surface currents at the unperturbed interface;

(B) the interface supports free-surface currents.

In formulating Maxwell's equations, we assume that the magneto-quasistatic approximation is valid for the system (Melcher 1963). Accordingly Maxwell's equations reduce to

$$\boldsymbol{\nabla}\cdot\mu\mathbf{H} = 0, \tag{2.2}$$

$$\boldsymbol{\nabla}\times\mathbf{H} = \begin{cases} 0 & \text{in case A,} \\ J_f & \text{in case B,} \end{cases} \tag{2.3}$$

where J_f is the surface current density (see Melcher 1963, p. 41, equation 3.51). In accordance with the validity of the quasistatic approximation, a stream function $\psi(r,\theta,t)$ can be introduced such that the total magnetic field is given by

$$\mathbf{H} = \frac{1}{r}\frac{\partial\psi}{\partial\theta}\mathbf{e}_r - \left(\frac{\partial\psi}{\partial r} - H_j\cos\tilde{\omega}t\right)\mathbf{e}_\theta, \tag{2.4}$$

where $\psi(r,\theta,t)$ is the increment in the magnetic field. Clearly, the stream function ψ guarantees that (2.2) is satisfied, while the remaining bulk equation ($\boldsymbol{\nabla}\times\mathbf{H} = 0$) shows that the function ψ satisfies Laplace's equation

$$\nabla^2\psi = 0. \tag{2.5}$$

Because the fluid is supposed to be non-conducting, the magnetic forces only act on interfaces. Their contribution appears in the normal component of the stress term in the boundary condition at the surface of separation. However, in the bulk, the volume equation is $\boldsymbol{\nabla}(\frac{1}{2}\mu H^2) = 0$, and so there is no contribution – there is an impulse at the boundaries, which is treated as a modification to the interfacial pressure: $\tilde{\pi} = P + \frac{1}{2}\mu H^2$, where P is the hydrostatic pressure. Thus the equation governing the behaviour for a non-rotating frame of reference for viscous fluids is

$$\left[\rho\frac{\partial}{\partial t}\mathbf{V} + \rho(\mathbf{V}\cdot\boldsymbol{\nabla})\,\mathbf{V} + \boldsymbol{\nabla}\tilde{\pi}\right] = \eta\nabla^2\mathbf{V}, \tag{2.6}$$

where $\mathbf{V}$ is the fluid velocity vector and η is the viscosity coefficient.

In the rotating frame of reference, the Coriolis term $2\boldsymbol{\Omega}\times\mathbf{V}$ is usefully introduced in the equation of motion. $\mathbf{V} = (\tilde{u}, \tilde{v}, \tilde{w})$, with $\tilde{u} = u$, $\tilde{v} = v$ and $\tilde{w} = 0$, is the total velocity of a fluid particle inside and outside the fluid column,

https://doi.org/10.1017/S0022377801001003 Published online by Cambridge University Press

where $(u, v, 0)$ are the perturbation velocity components. Consequently, the kinematic boundary condition at the interface for a moving fluid particle is given by

$$\frac{\partial \xi}{\partial t} = u_j \qquad (r = R) \tag{2.7}$$

However, in the present work, the Kelvin–Helmholtz model is adopted, so that the total velocity vector $\mathbf{V}$ is represented by $\mathbf{V} = (\tilde{u}, \tilde{v}, \tilde{w})$ with $\tilde{u} = u$, $\tilde{v} = v_0 + v$ and $\tilde{w} = 0$, where $v_0 = r\Omega$ is the unperturbed velocity. Consequently, the equation of motion is (2.6) and the kinematic boundary condition (2.7) is modified to

$$\frac{\partial \xi}{\partial t} = u_j - \Omega_j \frac{\partial \xi}{\partial \theta} \qquad (r = R) \tag{2.8}$$

In this work, we confine our analysis to weak viscous effects. These effects are believed to be significant only within a thin vortical surface layer, so that the motion elsewhere in the liquid column may reasonably be assumed to be irrotational. Thus the viscous effects are introduced through the normal damped stress term in the boundary condition at the surface of separation.

In view of the weakly viscous approximation, which is considered here, the governing equations for the bulk fluid phases are

$$\frac{\partial \tilde{u}}{\partial t} + \tilde{u}\frac{\partial \tilde{u}}{\partial r} + \frac{\tilde{v}}{r}\frac{\partial \tilde{u}}{\partial \theta} - \frac{\tilde{v}^2}{r} = -\frac{1}{\rho}\frac{\partial P}{\partial r}, \tag{2.9}$$

$$\frac{\partial \tilde{v}}{\partial t} + \tilde{u}\frac{\partial \tilde{v}}{\partial r} + \frac{\tilde{v}}{r}\frac{\partial \tilde{v}}{\partial \theta} + \frac{\tilde{v}\tilde{u}}{r} = -\frac{1}{\rho r}\frac{\partial P}{\partial \theta}, \tag{2.10}$$

$$\frac{\partial \tilde{w}}{\partial t} + \tilde{u}\frac{\partial \tilde{w}}{\partial r} + \frac{\tilde{v}}{r}\frac{\partial \tilde{w}}{\partial \theta} = -\frac{1}{\rho}\frac{\partial P}{\partial z}, \tag{2.11}$$

where cylindrical polar coordinates (r, θ, z) are used. The continuity equation $\boldsymbol{\nabla}\cdot\mathbf{V} = 0$ takes the form

$$\frac{\partial \tilde{u}}{\partial r} + \frac{1}{r}\frac{\partial \tilde{v}}{\partial \theta} + \frac{\partial \tilde{w}}{\partial z} + \frac{\tilde{u}}{r} = 0. \tag{2.12}$$

Owing to the assumption that the fluid performs irrotational motion, the velocity may be expressed as the gradient of a velocity potential $\phi(r, \theta, t)$, which, owing to the incompressibility condition $\boldsymbol{\nabla}\cdot\mathbf{V} = 0$, is a solution of Laplace's equation

$$\nabla^2\phi(r, \theta, t) = 0. \tag{2.13}$$

In the equilibrium state, the pressure is given by

$$P_j^{(0)} = \tfrac{1}{2}\rho_j r^2\Omega_j^2 + C_j, \tag{2.14}$$

where the superscript (0) refers to the equilibrium state, and C_j, $j = 1, 2$, are constants of integration. From the continuity of the normal stress at the interface, we find the jump in the pressure to be zero, whence

$$C_1 - C_2 = \frac{T}{R} + \tfrac{1}{2}R^2(\rho_2\Omega_2^2 - \rho_1\Omega_1^2) - \tfrac{1}{2}(\mu_1 H_1^2 - \mu_2 H_2^2)\cos^2\tilde{\omega}t, \tag{2.15}$$

https://doi.org/10.1017/S0022377801001003 Published online by Cambridge University Press

3. Boundary conditions

For the system adopted here, the following two types of boundary conditions are appropriate: conditions at an infinite distance from the system and conditions at the dividing surface. The former express the requirements that the magnetic field and the velocity vector tend to zero at infinity. The interfacial boundary conditions that must be satisfied at the surface $r = R$ are as follows:

(1) At the boundary between two fluids, the fluid and magnetic stresses must balance. The stress balance will be written using stress tensor form, and the derivation will follow that of Melcher (1963):

$$[\![\sigma_{ij}]\!]\, n_j = -T(\boldsymbol{\nabla}\cdot\mathbf{n})\, n_i, \tag{3.1}$$

where $[\![\ ]\!]$ represents the jump from region 1 to region 2, n_i and n_j are the components of a unit vector $\mathbf{n}$, and T is the surface-tension coefficient. The components of these stresses consist of the hydrodynamic pressure, viscous stresses and magnetic stresses:

$$\sigma_{rr} = -P + \tfrac{1}{2}\mu(H_r^2 - H_\theta^2) + 2\eta\frac{\partial\tilde{u}}{\partial r}, \tag{3.2}$$

$$\sigma_{\theta\theta} = -P - \tfrac{1}{2}\mu(H_r^2 - H_\theta^2) + 2\eta\left(\frac{\tilde{u}}{r} + \frac{1}{r}\frac{\partial\tilde{v}}{\partial\theta}\right), \tag{3.3}$$

$$\sigma_{r\theta} = \mu H_r H_\theta + \eta\left[\frac{1}{r}\frac{\partial\tilde{u}}{\partial\theta} + r\frac{\partial}{\partial r}\left(\frac{\tilde{v}}{r}\right)\right], \tag{3.4}$$

with σ_{ii} the normal stress and $\sigma_{r\theta}$ the shear stress.

(2) The kinematic boundary condition due to continuity at the surface is assumed.

(3) The normal component of the magnetic displacement is assumed to be continuous at the interface.

(4) The continuity of the tangential component of the magnetic field is assumed in the case where there are no free-surface currents at the interface.

(5) Owing to the presence of surface currents on the column interface, the tangential component of the magnetic field is discontinuous. Therefore the continuity of the tangential stress is assumed (Melcher 1963).

4. Linearized equations

To test the stabilization of the column system, the column radius will be assumed to be perturbed about its equilibrium value. The column radius is now given by

$$r = R + \xi(\theta, t), \tag{4.1}$$

where

$$\xi(\theta, t) = \gamma(t)\, e^{im\theta} \qquad (0 \leqslant \theta \leqslant 2\pi). \tag{4.2}$$

Here $\gamma(t)$ is an unknown function of time t, representing the amplitude of the

https://doi.org/10.1017/S0022377801001003 Published online by Cambridge University Press

perturbations in the column radius, and the integer m is the azimuthal wavenumber. The limiting case of very long longitudinal wavelength is considered here, so that the dependence of the variables on z will be neglected.

The equations of motion and boundary conditions given previously will be solved for these perturbations under the assumption that the perturbations are small; that is, all equations and boundary conditions will be linearized in the perturbation quantities. The form of the azimuthal variation for all the other perturbation variables will be the same as that of the radius description (4.2). The perturbation bulk variables are functions of both the azimuthal and the radial coordinates as well as time. Accordingly, the linearized velocity potential ϕ and the stream function ψ are governed by the following equations:

$$\left(r^2\frac{\partial^2}{\partial r^2}+r\frac{\partial}{\partial r}-m^2\right)\phi=0, \tag{4.3}$$

$$\left(r^2\frac{\partial^2}{\partial r^2}+r\frac{\partial}{\partial r}-m^2\right)\psi=0, \tag{4.4}$$

The increment of the pressure $\pi(r,\theta,t)$ is given by

$$\pi(r,\theta,t)=-\rho\left(\frac{\partial\phi}{\partial t}-\frac{2i\Omega}{m}r\frac{\partial\phi}{\partial r}+im\Omega\phi\right). \tag{4.5}$$

Equation (4.3) has to be solved with the following appropriate kinematic boundary condition:

$$\frac{\partial\phi_j}{\partial r}=\frac{\partial\xi}{\partial t}+im\Omega_j\xi \qquad (r=R) \tag{4.6}$$

Thus the velocity potentials $\phi_j(r,\theta,t)$, $j=1,2$, inside and outside the fluid column are given by

$$\phi_1(r,\theta,t)=\frac{R}{m}\left(\frac{r}{R}\right)^m\left(\frac{d\gamma}{dt}+im\Omega_1\gamma\right)e^{im\theta} \qquad (r\leqslant R), \tag{4.7}$$

$$\phi_2(r,\theta,t)=-\frac{R}{m}\left(\frac{R}{r}\right)^m\left(\frac{d\gamma}{dt}+im\Omega_2\gamma\right)e^{im\theta} \qquad (r\geqslant R). \tag{4.8}$$

In solving (4.4), with the appropriate boundary conditions, we shall deal with two different cases, depending on whether or not the unperturbed interface supports free-surface currents.

5. Case A: no free-surface currents at the column interface

This section deals with the case where the unperturbed interface $r=R$ is assumed to support no free-surface currents, so that in the equilibrium configuration, $H_1=H_2=H_0$. The appropriate magnetic boundary conditions that must be satisfied at the surface $r=R$ are as follows:

(1) the tangential component of the magnetic field is continuous at the interface; therefore

$$\frac{\partial\psi_1}{\partial r}-\frac{\partial\psi_2}{\partial r}=0 \qquad (r=R); \tag{5.1}$$

https://doi.org/10.1017/S0022377801001003 Published online by Cambridge University Press

(2) the normal component of the magnetic displacement is continuous at the interface; therefore

$$\left(\mu_1\frac{\partial\psi_1}{\partial\theta}-\mu_2\frac{\partial\psi_2}{\partial\theta}\right)-\frac{\partial\xi}{\partial\theta}(\mu_1-\mu_2)\,H_0\cos\tilde{\omega}t=0. \qquad (r=R). \tag{5.2}$$

With these boundary conditions, the solutions of Laplace's equation (4.4) yield the distribution of the stream function inside and outside the column as

$$\psi_1(r,\theta,t)=\frac{\mu_1-\mu_2}{\mu_1+\mu_2}\left(\frac{r}{R}\right)^m\gamma(t)\,H_0\cos\tilde{\omega}t\,e^{im\theta} \qquad (r\leqslant R), \tag{5.3}$$

$$\psi_2(r,\theta,t)=-\frac{\mu_1-\mu_2}{\mu_1+\mu_2}\left(\frac{r}{R}\right)^{-m}\gamma(t)\,H_0\cos\tilde{\omega}t\,e^{im\theta} \qquad (r\geqslant R). \tag{5.4}$$

It is well known that for inviscid fluids, the presence of a jump in the tangential stress is equivalent to continuity of the normal component of the magnetic field, since there are no free surface currents at the interface. In contrast, in the presence of viscosity, there is no such equivalence. Therefore it is necessary to take account of this boundary condition, which was neglected before. There are two further linearized boundary conditions: the continuity of the tangential stress and the discontinuity of the normal stress, which is related to the value of the surface-tension force. These conditions are respectively

$$\frac{1}{r}\frac{\partial\xi}{\partial\theta}([\![\sigma_{rr}]\!]-[\![\sigma_{\theta\theta}]\!])+[\![\sigma_{r\theta}]\!]=0 \qquad (r=R) \tag{5.5}$$

$$[\![\sigma_{rr}]\!]=-\frac{T}{r}+\nabla^2\xi(\theta,t) \qquad (r=R) \tag{5.6}$$

In view of the relations (3.1)–(3.4), the linearized tangential and normal stress components respectively reduce to

$$\left(\mu_1\frac{\partial\psi_1}{\partial\theta}-\mu_2\frac{\partial\psi_2}{\partial\theta}\right)H_0\cos\tilde{\omega}t-\frac{\partial\xi}{\partial\theta}(\mu_1-\mu_2)\,H_0^2\cos^2\tilde{\omega}t$$
$$+2\eta_1\frac{\partial}{\partial\theta}\left(\frac{\partial\phi_1}{\partial r}-\frac{1}{r}\phi_1\right)-2\eta_2\frac{\partial}{\partial\theta}\left(\frac{\partial\phi_2}{\partial r}-\frac{1}{r}\phi_2\right)=0 \qquad (r=R), \tag{5.7}$$

$$\pi_1-\pi_2=R(\rho_2\,\Omega_2^2-\rho_1\,\Omega_1^2)\,\xi+\frac{T}{R^2}(m^2-1)\,\xi-\left(\mu_1\frac{\partial\psi_1}{\partial r}-\mu_2\frac{\partial\psi_2}{\partial r}\right)H_0\cos\tilde{\omega}t$$
$$+2\eta_1\frac{\partial^2\phi_1}{\partial r^2}-2\eta_2\frac{\partial^2\phi_1}{\partial r^2} \qquad (r=R). \tag{5.8}$$

These conditions can be used to determine the dispersion relation that describes the behaviour of the surface wave. Substituting both the stream function $\psi_j(r,\theta,t)$ and the velocity potential $\phi_j(r,\theta,t)$ as obtained from the appropriate boundary conditions into (5.7), we obtain

$$[\eta_2(m+1)-\eta_1(m-1)]\frac{d\gamma}{dt}+im[\eta_2\,\Omega_2(m+1)-\eta_1\,\Omega_1(m-1)]\,\gamma=0, \tag{5.9}$$

https://doi.org/10.1017/S0022377801001003 Published online by Cambridge University Press

Although the continuity of the tangential stress is satisfied identically in inviscid fluids, (5.9) fails to be satisfied in the presence of viscosity, for

$$\eta_2(m+1)-\eta_1(m-1)=0, \qquad \Omega_1=\Omega_2\geqslant 0.$$

Consequently, the tangential stress makes no contribution in the case of low viscosity. Otherwise, the continuity of the tangential stress must be taken into account.

The normal stress component in terms of the perturbation amplitude $\gamma(t)$ is

$$\begin{aligned}
&\frac{d^2\gamma}{dt^2}+\frac{2}{R^2(\rho_1+\rho_2)}\{m[\eta_2(m+1)+\eta_1(m-1)]\\
&\quad+iR^2[\rho_2\,\Omega_2(m+1)+\rho_1\,\Omega_1(m-1)]\}\frac{d\gamma}{dt}\\
&\quad+\frac{1}{R^2(\rho_1+\rho_2)}\left\{\frac{m(m^2-1)T}{R}-mR^2[\rho_2\,\Omega_2^2(m+1)+\rho_1\,\Omega_1^2(m-1)]\right.\\
&\quad\left.+2im^2[\eta_2\,\Omega_2(m+1)+\eta_1\,\Omega_1(m-1)]+\frac{m^2(\mu_2-\mu_1)^2\mathrm{H}_0^2}{(\mu_2+\mu_1)}\cos^2\tilde{\omega}t\right\}\gamma=0, \qquad (5.10)
\end{aligned}$$

which is a second-order differential equation of Mathieu type with complex coefficients. In the limiting case for a non-rotating fluid column, the above equation reduces to the damping Mathieu equation with real coefficients. For non-vanishing angular velocity Ω_j, the damped Mathieu equation can also be obtained. This may be accomplished by using (5.9) to eliminate the coefficients of the imaginary terms appearing in (5.10). This approach leads to a single damped Mathieu equation, which represents the dispersion relation and controls the behaviour of the viscous effects in surface-wave instability. Thus the system will be governed by the following equation:

$$\frac{d^2\gamma}{dt^2}+\alpha\frac{d\gamma}{dt}+(\delta+QH_0^2\cos^2\tilde{\omega}t)\,\gamma=0, \qquad (5.11)$$

where

$$\begin{aligned}
\delta&=\frac{m}{\rho_1+\rho_2}\left\{\frac{(m^2-1)\,T}{R^3}+\frac{2\Omega_1\,\Omega_2(\rho_1\,\eta_2-\rho_2\,\eta_1)\,(m^2-1)}{\eta_2(m+1)-\eta_1(m-1)}\right.\\
&\quad\left.+\frac{[\rho_2\,\Omega_2^2(m+1)-\rho_1\,\Omega_1^2(m-1)]\,[\eta_2(m+1)+\eta_1(m-1)]}{\eta_2(m+1)-\eta_1(m-1)}\right\},\\
\alpha&=\frac{4m(m^2-1)\,(\Omega_2-\Omega_1)\,\eta_1\,\eta_2}{R^2(\rho_1+\rho_2)\,[\eta_2\,\Omega_2(m+1)-\eta_1\,\Omega_1(m-1)]},\\
Q&=\frac{m^2\mu^*}{R^2(\rho_1+\rho_2)}, \qquad \mu^*=\frac{(\mu_2-\mu_1)^2}{\mu_2+\mu_1}.
\end{aligned}$$

Equation (5.11) has a growth-rate solution, and stability requires positive values of the damped term. The periodic solution arises when the damped term vanishes. In the case of equal angular velocities, we can obtain a periodic

https://doi.org/10.1017/S0022377801001003 Published online by Cambridge University Press

solution even in the presence of viscosity. The Mathieu equation (5.11) then reduces to

$$\frac{d^2\gamma}{dt^2}+(\delta_0+QH_0^2\cos^2\tilde{\omega}t)\,\gamma=0, \tag{5.12}$$

where

$$\delta_0=\frac{m}{\rho_1+\rho_2}\left\{\frac{(m^2-1)\,T}{R^3}+\Omega_0^2[\rho_2(m+1)+\rho_1(m-1)]\right\}, \tag{5.13}$$

Although the viscosity coefficients η_1 and η_2 have disappeared from (5.12), we conclude that this equation still governs the behaviour of the viscous fluid interface in the marginal state where $\Omega_1=\Omega_2=\Omega_0$.

Note that in the case of a static magnetic field, both the angular velocity and the magnetic field make no contribution in the stabilized problem. In the case of non-vanishing field frequency $\tilde{\omega}$, stability occurs when the following inequality is satisfied:

$$H_0^4Q^2+16(\tilde{\omega}^2-\delta_0)\,QH_0^2+32\delta_0(\tilde{\omega}^2-\delta_0)>0. \tag{5.14}$$

This stability criterion reduces to the problem of the bounded regions of the Mathieu functions, as given in McLachlan (1964). It is observed that this condition is trivially satisfied when $\tilde{\omega}^2\geqslant\delta_0$, for arbitrary Q and H_0^2. In terms of the magnetic field H_0^2, the above stability condition (5.14) takes the form

$$(H_0^2-H_1^*)\,(H_0^2-H_2^*)>0, \tag{5.15}$$

where

$$H_{1,2}^*=\frac{8}{Q}[-(\tilde{\omega}^2-\delta_0)\pm\sqrt{(\tilde{\omega}^2-\delta_0)\,(\tilde{\omega}^2-\tfrac{3}{2}\delta_0)}]. \tag{5.16}$$

The stable regions are characterized by the following conditions:

$$H_0^2>H_1^* \quad \text{and} \quad H_0^2<H_2^* \quad (H_1^*>H_2^*). \tag{5.17}$$

From Floquet theory (McLachlan 1964), the region bounded by the two branches for the transition curves H_1^* and H_2^* is the unstable region; the area outside these curves is the stable region. Thus the width of the unstable region is measured by the difference $H_1^*-H_2^*$. The effect of the angular velocity Ω_0 on this width is determined from the sign of

$$\frac{\partial}{\partial\Omega_0}(H_1^*-H_2^*)=\frac{4(6\delta_0-5\tilde{\omega}^2)}{Q\sqrt{(\tilde{\omega}^2-\delta_0)\,(\tilde{\omega}^2-\frac{3}{2}\delta_0)}}\frac{\partial\delta_0}{\partial\Omega_0}. \tag{5.18}$$

A positive sign of this quantity means that an increase in the angular velocity increases the size of the unstable region. It is easy to show that the sign of this quantity depends on the term $6\delta_0-5\tilde{\omega}^2$. Thus an increase in the size of the unstable region with increasing Ω_0 requires that

$$6\delta_0-5\tilde{\omega}^2>0.$$

Using (4.13), the above condition reduces to

$$\Omega_0^2>\frac{\rho_1+\rho_2}{6m[\rho_2(m+1)+\rho_1(m-1)]}\left[5\tilde{\omega}^2-\frac{6m}{\rho_1+\rho_2}(m^2-1)\,T\right], \tag{5.19}$$

It is clear that the above inequality is trivially satisfied in the absence of the

https://doi.org/10.1017/S0022377801001003 Published online by Cambridge University Press

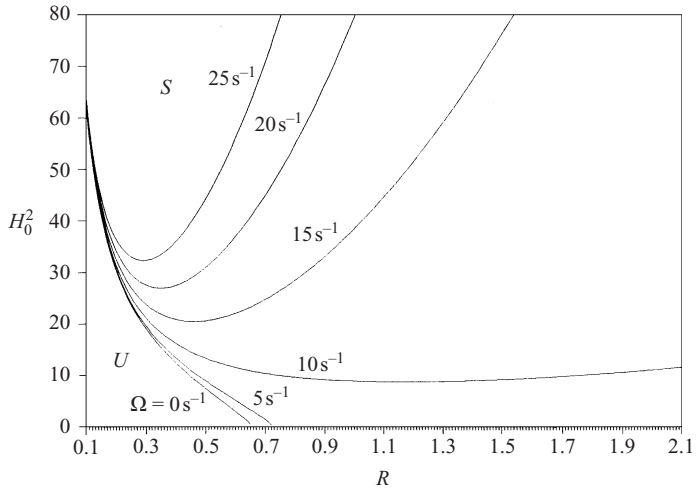

Figure 1. Stability diagram for a system having $\rho_1 = 0.879$ g cm^{-3}, $\rho_2 = 0.99823$ g cm^{-3}, $T = 35$ dyn cm^{-1} and $\mu^* = 148$. The graph indicates the transition curve H_1^* given by (5.16), while the transition curve H_2^* has negative values. The region labelled S is the stable region. The region labelled by U is the unstable region.

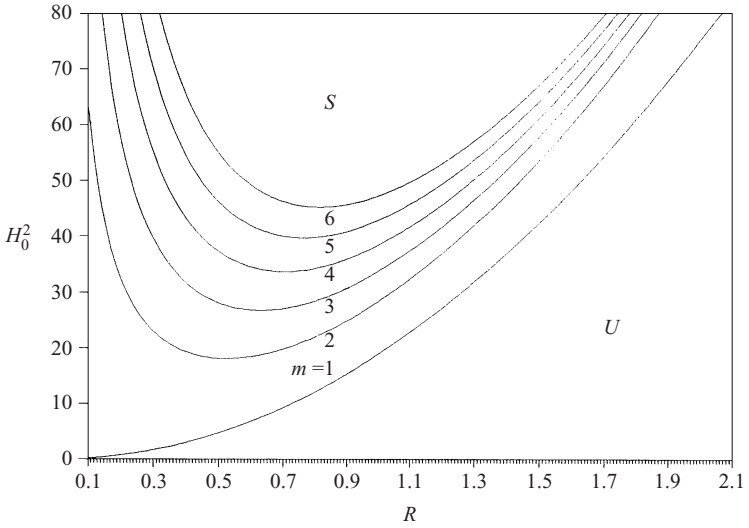

Figure 2. Stability diagram for the same system as in Fig. 1, but with $\tilde{\omega} = 5$ Hz.

field frequency $\tilde{\omega}$, which shows the destabilizing role of the angular velocity Ω_0. The presence of the frequency $\tilde{\omega}$ retards this destabilizing influence. As the values of the frequency $\tilde{\omega}$ increases larger values of Ω_0 are required to produce the same destabilizing effect.

A numerical illustration of the stability condition (5.14) is shown in Figs 1–3 for a system having $\rho_1 = 0.879$ g cm^{-3}, $\rho_2 = 0.99823$ g cm^{-3}, $T = 35$ dyn cm^{-1} and $\mu^* = 148$.

It is apparent from these figures that an increase in the magnetic field H_0^2 as well as an increase in the column radius R has a stabilizing influence. This

https://doi.org/10.1017/S0022377801001003 Published online by Cambridge University Press

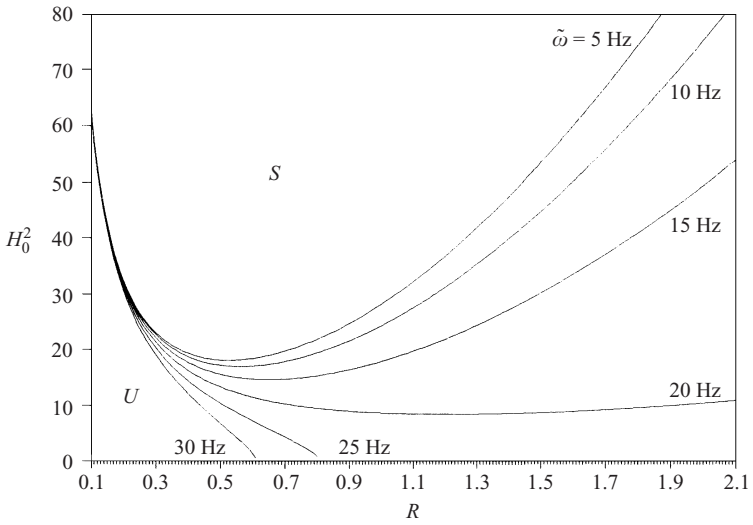

Figure 3. Stability diagram for the same system as in Fig. 1, with the angular velocity and azimuthal wavenumber are held fixed ($\Omega = 10$ and $m = 2$).

stabilizing role is affected by increasing angular velocity Ω, azimuthal wavenumber m and field frequency $\tilde{\omega}$.

It is readily seen from Fig. 1 that there is a zone of stability bounded by the transition curve H_1^* for $m = 2$ and $\tilde{\omega} = 20$ Hz. The calculation has been done, varying Ω from 0 s^{-1} to 25 s^{-1} with step 5 s^{-1}. This stable zone decreases in size as the angular velocity Ω is increased. It is observed that for small values of Ω, the transition curve intersects the R axis. On increasing Ω, the stable zone contracts, and leaves the R axis. This shows the destabilizing influence of Ω on the stability criteria.

In Fig. 2, we plot the magnetic field H_0^2 versus the column radius R for the same system as in Fig. 1, but with $\tilde{\omega} = 5$ Hz. The transition curve H_1^* is given for $m = 1, \ldots, 6$. The stability region decreases in size as R is increased. As m is increased, larger values of H_0^2 are needed to produce the same stability configuration. This shows the destabilizing influence of increasing m.

The diagram shown in Fig. 3 is for the same system as in Fig. 1, with the angular velocity and azimuthal wavenumber held fixed ($\Omega = 10$ s^{-1} and $m = 2$), with the field frequency $\tilde{\omega}$ being varied from 5 Hz to 30 Hz with step 5 Hz. Inspection of this graph shows that increasing $\tilde{\omega}$ increases the size of the stable zone. It can be seen that the field frequency $\tilde{\omega}$ plays a counteracting role to the angular velocity Ω.

In this section, the stability behaviour has been examined for matching angular velocities. As the angular velocities are matched, the viscosity coefficients η_1 and η_2 disappear from the stability condition (5.14). It can be seen that this condition does not hold for the corresponding case in the inviscid problem. Therefore the viscosity contribution is associated with the presence of a difference in angular velocities. The field frequency then plays a stabilizing role, while increasing the azimuthal wavenumber m and equal angular velocities have a destabilizing influence.

https://doi.org/10.1017/S0022377801001003 Published online by Cambridge University Press

5.1. Stability behaviour due to a non-vanishing damping term α

A singular case occurs when the denominators of both coefficients δ and α have zero value. This means that there exists a critical value of the stratified viscosity η $(=\eta_1/\eta_2)$ that leads to this singular case. That is,

$$\eta=\frac{m+1}{m-1} \quad \text{and} \quad \eta=\frac{m+1}{\Omega(m-1)}, \quad m\neq 1, \quad \Omega=\frac{\Omega_1}{\Omega_2}.$$

Such singularities disappear in the case of periodic solutions, i.e. in the case of a non-rotating fluid column or when the angular velocities are equal.

We shall deal with the non-singular case, ignoring the critical values of η. Therefore, as the coefficient α has non-zero values in (5.11), a growth-rate disturbance occurs. There are many books that have treated (5.11) (see e.g. Grimshaw 1990). The small and positive coefficient α is described as a function of the coefficient of the period term.

In a static magnetic field, (5.11) reduces to

$$\frac{d^2\gamma}{dt^2}+\alpha\frac{d\gamma}{dt}+(\delta+QH_0^2)\,\gamma=0, \tag{5.20}$$

which is a linear differential equation with constant coefficients, and can be satisfied by a growth rate solution having the form $\gamma=\exp(\sigma+i\omega)t$. The stability will depend on the sign of σ (the real part). If it is positive then the amplitude of the disturbance increases with time, and the flow is unstable; if it is negative then the flow is stable; and if it has a zero value then there is marginal stability. Both σ and ω are real constants and satisfy the following equations:

$$\sigma^2-\omega^2+\alpha\sigma+(\delta+QH_0^2)=0, \qquad 2\sigma+\alpha=0.$$

Elimination of the parameter σ yields

$$\omega^2=\delta+QH_0^2-\tfrac{1}{4}\alpha^2. \tag{5.21}$$

The assumption that ω is real imposes the following stability condition:

$$\delta+QH_0^2-\tfrac{1}{4}\alpha^2>0, \tag{5.22}$$

with the necessary condition that α is positive. Thus the region of stability in the static case is given by

$$H_0^2>H_0^*=\frac{1}{4Q}(\alpha^2-4\delta). \tag{5.23}$$

The presence of the damping term α in the stability analysis that is given above leads us to estimate the contribution of the viscosity in the stability criteria. Therefore a non-dimensional parameter η^* is introduced such that $\eta_j=\eta^*\tilde{\eta}_j$, and then $\alpha=\eta^*\tilde{\alpha}$. The dependence of the transition curve H_0^* with respect to η^* is given by

$$\frac{\partial H_0^*}{\partial\eta^*}=\frac{\tilde{\alpha}^2}{2Q}\eta^*>0. \tag{5.24}$$

This means that the unstable region bounded by the curve H_0^* is increased in size as η^* is increased, which shows that an increase in the viscosity parameter has a destabilizing influence.

https://doi.org/10.1017/S0022377801001003 Published online by Cambridge University Press

For a non-zero field frequency $\tilde{\omega}$, Grimshaw (1990) examined, using a perturbation technique, the first unstable region, which occurs near $\delta = (\tilde{\omega}^2 + \frac{1}{4}\alpha^2) - \frac{1}{2}QH_0^2$. On the boundaries of this unstable region, there are periodic solutions of (5.11) of period 2π. The stability condition is thus given by

$$3Q^2H_0^4 + 16(\delta - \tilde{\omega}^2)\,QH_0^2 + 16(\delta - \tilde{\omega}^2)^2 + 16\tilde{\omega}^2\alpha^2 > 0. \tag{5.25}$$

The presence of a positive damped term has not altered the position of the stability boundary for the undamped Mathieu equation in the stability diagram in the (δ, Q) plane. For each fixed $\alpha > 0$, in the (δ, Q) plane, there is a hyperbola bounding the unstable region. These boundaries are described by

$$\tilde{H}^*_{1,2} = \frac{4}{3Q}[2(\tilde{\omega}^2 - \delta) \pm \sqrt{(\tilde{\omega}^2 - \delta)^2 - 3\tilde{\omega}^2\alpha^2}]. \tag{5.26}$$

The two transition curves $\tilde{H}^*_1$ and $\tilde{H}^*_2$ will meet when the field frequency $\tilde{\omega}$ is such that the square root in (5.26) is zero, and thus, when the parameter α is zero, the curves meet when $\tilde{\omega}^2 = \delta$. The nearness of $\tilde{\omega}$ to $\delta^{1/2}$ produces the resonance case (Nayfeh and Mook 1979). Since the parameter $\delta^{1/2}$ represents the disturbance frequency for (5.20) as $\alpha \to 0$ and $H_0 \to 0$, it is clear that the viscous damping term α decreases the size of the unstable region that is sandwiched between the boundaries $\tilde{H}^*_1$ and $\tilde{H}^*_2$. We may further examine the behaviour of the unstable region between the transition curves $\tilde{H}^*_1$ and $\tilde{H}^*_2$. Thus

$$\frac{\partial}{\partial \eta^*}(\tilde{H}^*_1 - \tilde{H}^*_2) = \frac{-8\tilde{\omega}^2\tilde{\alpha}^2\eta^*}{Q\sqrt{(\tilde{\omega}^2 - \delta)^2 - 3\tilde{\omega}^2\alpha^2}} < 0. \tag{5.27}$$

This means that the size of the unstable zone decreases as η^* is increased, which shows the stabilizing influence of increasing η^*. Therefore it is apparent that there is a change of the viscosity mechanism in the presence of the field frequency $\tilde{\omega}$.

5.2. Numerical illustration in the presence of the damping term α

A numerical investigation has been carried out of the stability conditions (5.23) and (5.25) in the absence and in the presence of the field frequency $\tilde{\omega}$ respectively. The data for the graphs are the same as in Fig. 1, with $\Omega_1 = 10\ \mathrm{s}^{-1}$, $\Omega_2 = 8\ \mathrm{s}^{-1}$, $\tilde{\eta}_1 = 0.8\ \mathrm{g\ cm}^{-1}\ \mathrm{s}^{-1}$, $\tilde{\eta}_2 = 0.3\ \mathrm{g\ cm}^{-1}\ \mathrm{s}^{-1}$ and a field frequency $\tilde{\omega} = 10$ Hz. The results are displayed in Figs 4–6. Part (a) of each figure is for the case in which the field is independent of the time, while part (b) is for the case with a non-zero field frequency $\tilde{\omega}$.

In Fig. 4, graphs in the plane (H_0^2, R) are plotted for three values of the viscosity parameter η^*: 0, 5 and 10. The inviscid transition curves intersect the R axis. In Fig. 4(a), the intersection lies at $R = 0.5075002$ cm, while in Fig. 4(b), it occurs at $R = 0.4891101$ cm and represents the resonance point that is present for $\tilde{\omega}^2 \approx \delta$ (Nayfeh and Mook 1979). A damping role is observed for non-zero η^*. Inspection of these graphs show that there are two different roles appearing for the variation of η^*. There is a destabilizing influence with a damping role in the stable area where the static field is present, as shown in Fig. 4(a). Owing to the presence of the field frequency $\tilde{\omega}$, there is a stabilizing influence associated with a damping role in the unstable zone, as shown in Fig. 4(b).

https://doi.org/10.1017/S0022377801001003 Published online by Cambridge University Press

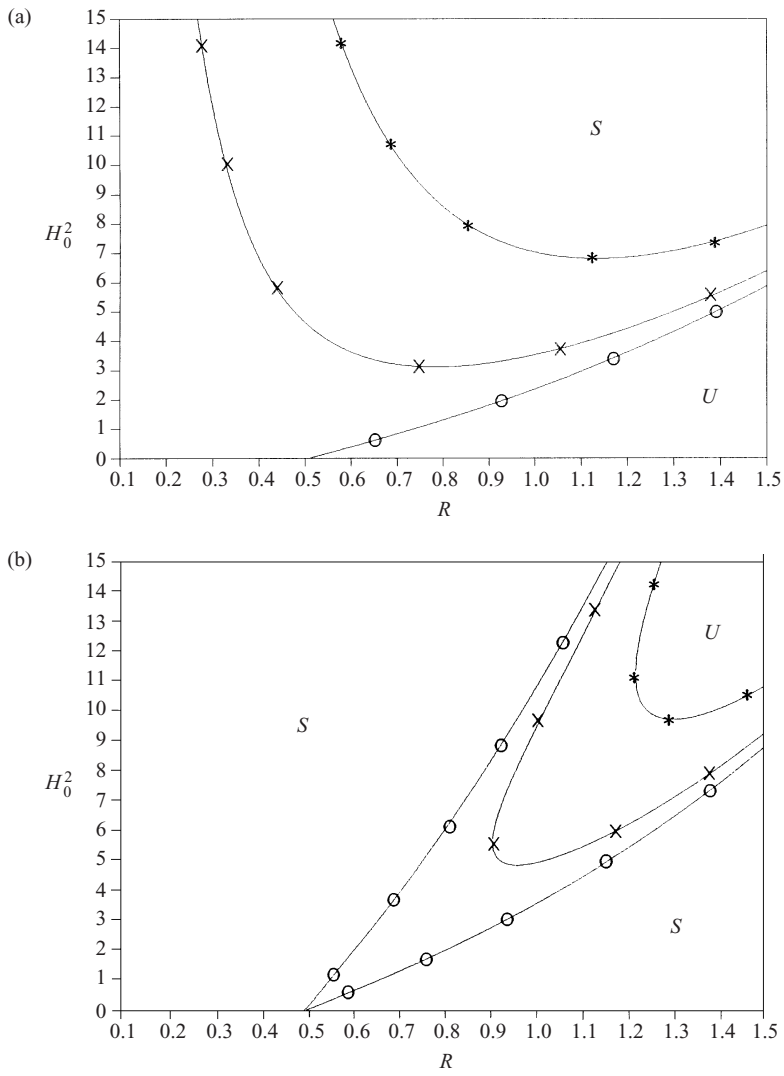

Figure 4. (a) The (H_0^2, R) plane for the stability condition (5.23). The data are the same as in Fig. 1, with $\Omega_1 = 10\ \mathrm{s}^{-1}$, $\Omega_2 = 8\ \mathrm{s}^{-1}$, $\tilde{\eta}_1 = 0.8\ \mathrm{g\ cm}^{-1}\ \mathrm{s}^{-1}$, $\tilde{\eta}_2 = 0.3\ \mathrm{g\ cm}^{-1}\ \mathrm{s}^{-1}$ and the field frequency $\tilde{\omega} = 10$ Hz. The curves are as follows: ○, $\eta^* = 0$ (the inviscid case); ×, $\eta^* = 5$; ●, $\eta^* = 10$. (b) is for the same system as in (a), except that the graphs are for the stability condition (5.25); the curves are labelled as in (a).

The damping parameter α is affected by the angular velocity Ω_j, and for α to be non-zero, we must have $\Omega_1 \neq \Omega_2$. Therefore a non-dimensional parameter Ω^* will be introduced such that $\Omega_1 = \Omega^*\tilde{\Omega}_1$ and $\Omega_2 = \Omega^*\tilde{\Omega}_2$. The effect of varying Ω^* ($\Omega^* = 1$, 2 and 3) is displayed in Fig. 5, where η^* is held fixed (equal to 5 in Fig. 5(a) and equal to zero in Fig. 5(b)). In Fig. 5(a), we find that the parameter Ω^* plays the same role as the parameter η^*, i.e. it has a destabilizing effect with a damping role in the stable zone in the case where the field is independent of time. Moreover, the intersection of the transition curve with the R axis in the case of $\eta^* = 0$ is affected by changes in the value of Ω^*. In Fig. 5(b), the

https://doi.org/10.1017/S0022377801001003 Published online by Cambridge University Press

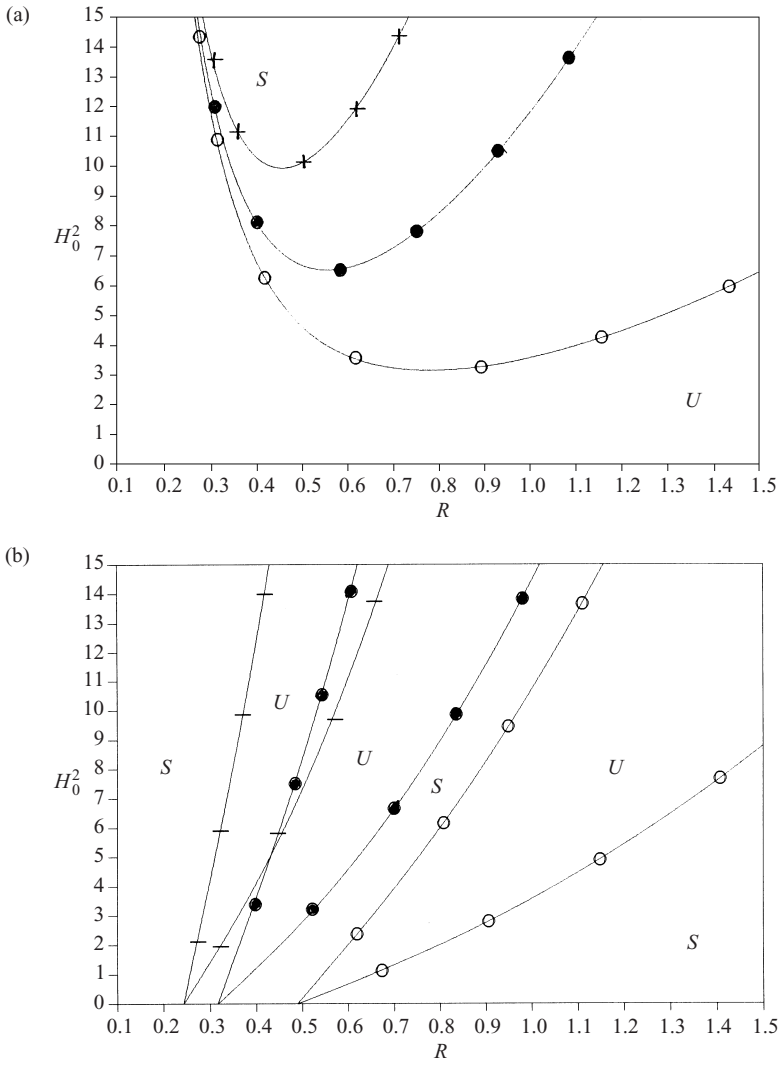

Figure 5. The (H_0^2, R) plane for the same system as in Fig. 4(a), with η^* is held fixed equal to 5: ○, $\Omega^* = 1$; ●, $\Omega^* = 2$; +, $\Omega^* = 3$. (b) is for the same stability condition as in Fig. 4(b), with η^* held fixed equal to zero; the curves are labelled as in (a).

resonance point is affected by an increase in Ω^*, and is shifted in the direction of decreasing R. It is located at $R = 0.4891101$ cm, 0.3166288 cm and 0.2429199 cm for $\Omega^* = 1$, 2 and 3 respectively. Again a stabilizing effect with a damping role in the unstable zone is found in the presence of the field frequency $\tilde{\omega}$. At this point, we can say that both the viscosity parameter η^* and the angular velocity Ω^* have changed their roles in the presence of the field frequency $\tilde{\omega}$. Proceeding from this, we can infer the effects of an increase in $\tilde{\omega}$ on the stability criteria in the presence of the damping term α. The viscous damping term α^2 in the stability condition (5.25) is multiplied by the parameter $\tilde{\omega}^2$. This shows that an increase of $\tilde{\omega}$ increases the stabilizing role played by η^*. Thus the frequency $\tilde{\omega}$ plays a stabilizing role, in agreement with the previous results as shown in Fig. 3.

https://doi.org/10.1017/S0022377801001003 Published online by Cambridge University Press

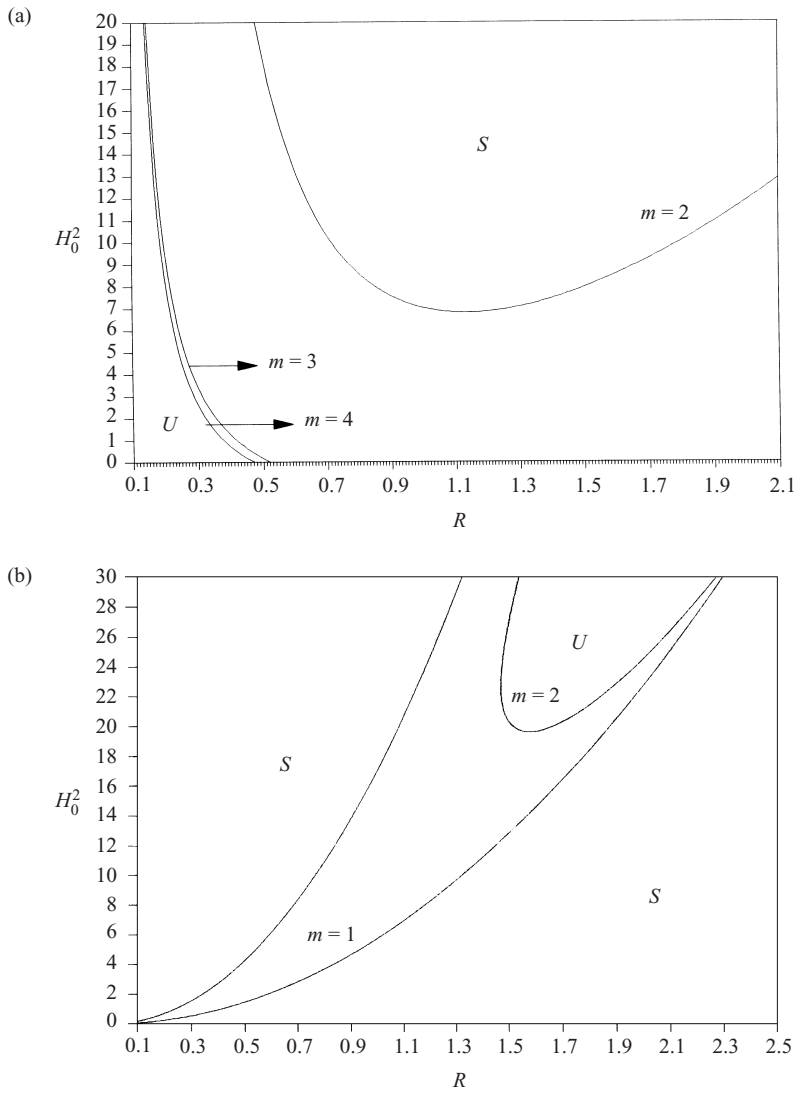

Figure 6. (a) The (H_0^2, R) plane for the same system as in Fig. 4(a), except that here $\tilde{\omega} = 20$ Hz. (b) As Fig. 4(b), except that here $\tilde{\omega} = 20$ Hz.

In Fig. 6, the (H_0^2, R) plane is shown for the same system as in Fig. 4, except that here $\tilde{\omega} = 20$ Hz. In Fig. 6(a), m has the values $m = 2$, 3 and 4, while in Fig. 6(b), the calculations are for $m = 1$ and 2. Inspection of these graphs shows that the stable region is increased in size as m is changed from 1 to 2. This stabilizing influence is not affected by the presence or absence of $\tilde{\omega}$. On the other hand, the presence of the parameter α leads to an opposite effect compared with that shown in Fig. 2. It can be noted in Fig. 6(b) that there is stability for the system when m is greater than 2, while in Fig. 6(a), we can see that there is stability when $m = 1$. The (H_0^2, R) plane is divided into a stable region and an unstable region when $m = 2$. An increase in m increases the size of the stable region.

https://doi.org/10.1017/S0022377801001003 Published online by Cambridge University Press

6. Case B: a viscous conducting interface supporting free-surface currents

This section is concerned with the presence of free-surface currents J_f on the interface $r = R$, so that $H_1 \neq H_2$. At the interface $r = R$, the magnetic boundary conditions that have to be satisfied can be summarized as follows. Owing to the presence of surface currents at the surface of separation, the continuity of the tangential field is irrelevant and only the continuity of the tangential stress (5.5) is applicable, while the continuity of the normal component of the displacement (5.2) still holds. Applying these boundary conditions to the bulk solution given by Laplace's equation (4.4), keeping in mind that $H_1 \neq H_2$, we obtain

$$\begin{aligned}\psi_1(r,\theta,t) = \frac{1}{m\mu_1(H_2-H_1)\cos\tilde{\omega}t}\left(\frac{r}{R}\right)^m\Big\{&2i[\eta_1(m-1)-\eta_2(m+1)]\frac{d\gamma}{dt}\\&-m[2\eta_1\Omega_1(m-1)-2\eta_2\Omega_2(m+1)\\&+i\mu_1 H_1(H_1-H_2)\cos^2\tilde{\omega}t]\,\gamma\Big\}e^{im\theta}\quad (r\leqslant R),\end{aligned}\tag{6.1}$$

$$\begin{aligned}\psi_2(r,\theta,t) = \frac{-1}{m\mu_2(H_2-H_1)\cos\tilde{\omega}t}\left(\frac{R}{r}\right)^m\Big\{&2i[\eta_1(m-1)-\eta_2(m+1)]\frac{d\gamma}{dt}\\&-m[2\eta_1\Omega_1(m-1)-2\eta_2\Omega_2(m+1)\\&+i\mu_2 H_2(H_1-H_2)\cos^2\tilde{\omega}t]\,\gamma\Big\}e^{im\theta}\quad (r\geqslant R).\end{aligned}\tag{6.2}$$

It is clear that the stream function ψ depends on the column radius, the angular velocity, the viscosity and the magnetic field.

In order to examine the behaviour of the surface current density in the stabilized problem, we assume the following equilibrium configuration:

$$H_1 = \frac{H}{H-1}J_f, \qquad H_2 = \frac{1}{H-1}J_f,\tag{6.3}$$

where H is the stratified magnetic field intensity ($H \equiv H_1/H_2$). Employing similar techniques to those used in case A to construct the characteristic equation, we find that the surface waves are governed by

$$\frac{d^2\gamma}{dt^2}+2(a_1+ib_1)\frac{d\gamma}{dt}+(a_2+2ib_2+qJ_f^2\cos^2\tilde{\omega}t)\,\gamma = 0,\tag{6.4}$$

where

$$a_1 = \frac{2m}{R^2(\rho_1+\rho_2)\,(H-1)}[H\eta_2(m+1)-\eta_1(m-1)],\tag{6.5}$$

$$a_2 = \frac{m}{(\rho_1+\rho_2)}\left\{\frac{(m^2-1)\,T}{R^3}-[\rho_2\Omega_2^2(m+1)+\rho_1\Omega_1^2(m-1)]\right\},\tag{6.6}$$

$$b_1 = \frac{1}{(\rho_1+\rho_2)}[\rho_2\Omega_2(m+1)+\rho_1\Omega_1(m-1)],\tag{6.7}$$

https://doi.org/10.1017/S0022377801001003 Published online by Cambridge University Press

$$b_2 = \frac{2m^2}{R^2(\rho_1+\rho_2)\,(H-1)}[H\eta_2\,\Omega_2(m+1)-\eta_1\,\Omega_1(m-1)], \tag{6.8}$$

$$q = \frac{m^2(\mu_1 H^2+\mu_2)}{R^2(\rho_1+\rho_2)\,(H-1)^2}. \tag{6.9}$$

Equation (6.4) is a second-order equation of Mathieu type with complex coefficients.

6.1. Stability behaviour for a viscous fluid column without rotation

The effect of the surface current density on a viscous fluid can be analysed in the limiting case as the angular velocity Ω_j vanishes; (6.4) then reduces to

$$\frac{d^2\gamma}{dt^2}+\left\{\frac{4m[H\eta_2(m+1)-\eta_1(m-1)]}{R^2(\rho_1+\rho_2)\,(H-1)}\right\}\frac{d\gamma}{dt}+\left[\frac{m(m^2-1)\,T}{R^3(\rho_1+\rho_2)}+qJ_f^2\cos^2\tilde{\omega}t\right]\gamma = 0, \tag{6.10}$$

which is a damped Mathieu equation with real coefficients. It is clear that there is a critical value for the stratified magnetic field for which the damping term is absent; this critical value is given by

$$H_c = \frac{\eta(m-1)}{m+1}, \tag{6.11}$$

where η is the stratified viscosity ($\eta \equiv \eta_1/\eta_2$). In the case where there is no frequency $\tilde{\omega}$, the stability analysis for Eq. (6.10) imposes the following condition (as in case A):

$$J_f^2 > J^*, \tag{6.12}$$

provided that the damping term has positive values, where

$$J^* = \frac{1}{mR(\mu_1 H^2+\mu_2)}\left\{\frac{4m}{R(\rho_1+\rho_2)}[H\eta_2(m+1)-\eta_1(m-1)]^2-(H-1)^2(m^2-1)\,T\right\}. \tag{6.13}$$

It is clear that the stability condition is trivially satisfied in the absence of viscosity η_j. The presence of η_j produces an unstable region bounded by the curve J^*. On the other hand, instability can be produced for values of H far from H_c. This unstable region increases in size as η_j is increased. At the critical value H_c of the stratified magnetic field, there is stability for all values of the surface current, i.e. the surface current J_f makes no contribution in this case. It is easy to show that as the column radius R is increased, the destabilizing role of viscosity is decreased and so the site of the unstable region that is bounded by J^* is decreased.

In the presence of the field frequency $\tilde{\omega}$, the stability boundaries have the form

$$\begin{aligned} J^*_{1,2} = \frac{4(H-1)}{3m^2(\mu_1 H^2+\mu_2)}\Bigg(&2(H-1)\left[R^2(\rho_1+\rho_2)\,\tilde{\omega}^2-\frac{m}{R}(m^2-1)\,T\right] \\ &\pm\Bigg\{(H-1)^2\left[R^2(\rho_1+\rho_2)\,\tilde{\omega}^2-\frac{m}{R}(m^2-1)\,T\right]^2 \\ &-48\tilde{\omega}^2m^2[H\eta_2(m+1)-\eta_1(m-1)]^2\Bigg\}^{1/2}\Bigg), \end{aligned} \tag{6.14}$$

https://doi.org/10.1017/S0022377801001003 Published online by Cambridge University Press

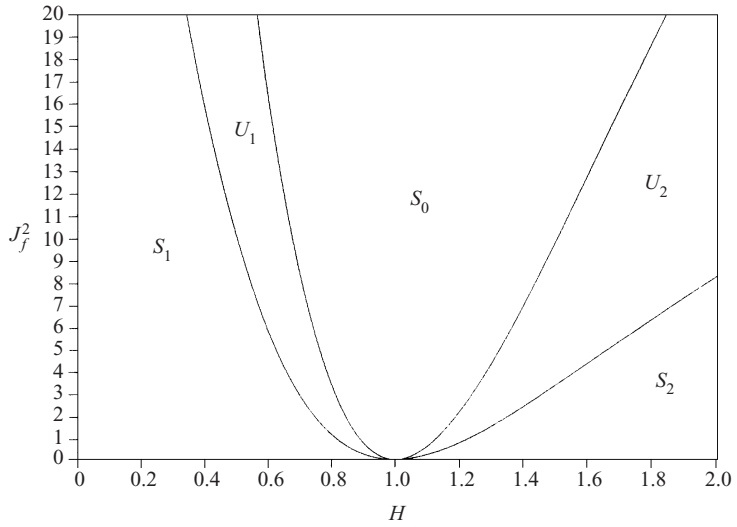

Figure 7. The transition curves (6.14) are plotted in the (J_f^2, H) plane for a system having $\eta_1 = 0.8$ g cm^{-1} s^{-1}, $\eta_2 = 0.3$ g cm^{-1} s^{-1}, $\rho_1 = 0.879$ g cm^{-3}, $\rho_2 = 0.99823$ g cm^{-3}, $T = 35$ dyn cm^{-1}, $\mu_1 = 14$, $\mu_2 = 9$, $R = 1.5$ cm, $m = 2$ and $\tilde{\omega} = 20$ Hz.

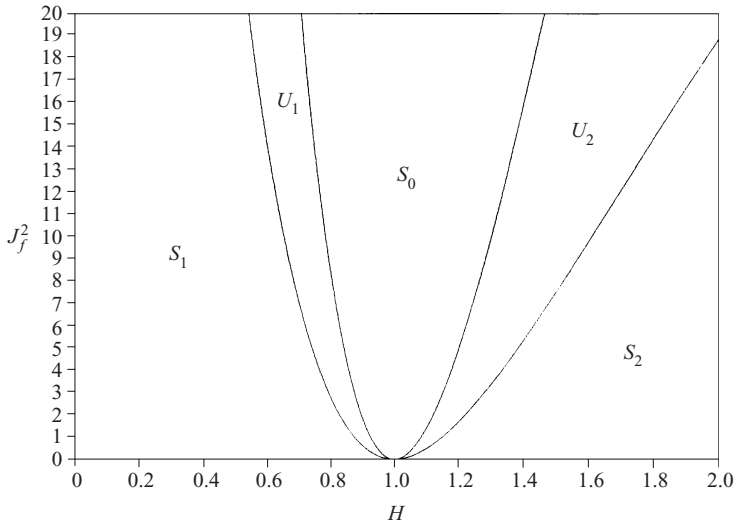

Figure 8. As in Fig. 7, but with $\tilde{\omega} = 30$ Hz.

where the stability criterion for the damped Mathieu equation (6.10) is given by (5.25) (Grimshaw 1990). Thus the stable region is characterized by

$$J_f^2 > J_1^* \quad \text{or} \quad J_f^2 < J_2^* \quad (J_1^* > J_2^*). \tag{6.15}$$

The transition curves (6.14) are plotted in the (J_f^2, H) plane for a sample case. The results of the calculations are shown in Figs 7–11 for a system having $\eta_1 = 0.8$ g cm^{-1} s^{-1}, $\eta_2 = 0.3$ g cm^{-1} s^{-1}, $\rho_1 = 0.879$ g cm^{-3}, $\rho_2 = 0.99823$ g cm^{-3}, $T = 35$ dyn cm^{-1}, $\mu_1 = 14$, $\mu_2 = 9$, $R = 1.5$ cm, $m = 2$ and $\tilde{\omega} = 20$ Hz.

https://doi.org/10.1017/S0022377801001003 Published online by Cambridge University Press

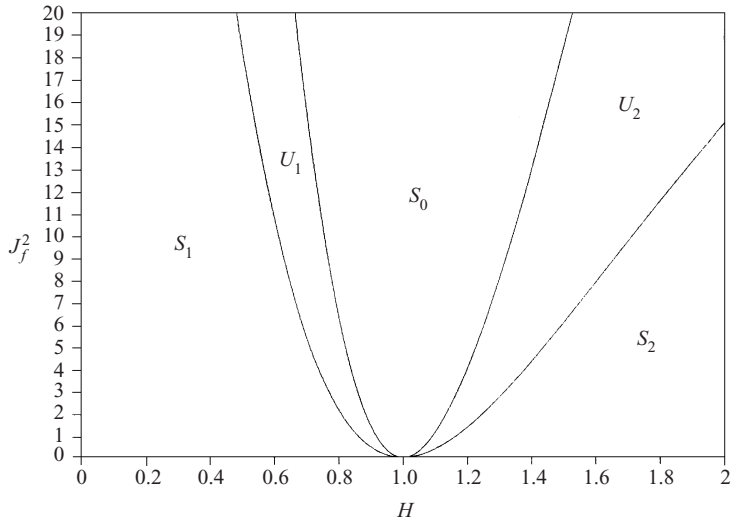

Figure 9. As in Fig. 7, but with $R = 2$ cm.

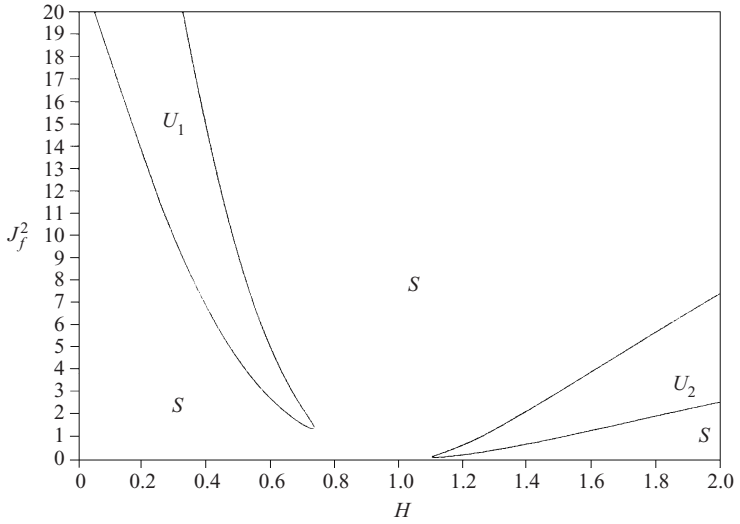

Figure 10. As in Fig. 7, but with $m = 3$.

It is readily seen from Fig. 7 that a coupled parametric resonance occurs in the neighbourhood of the point $H = 1$. The coupled resonance point depends on the specific values of m, η_1 and η_2. It is observed that this coupled resonance occurs at $\eta_2(m+1) = \eta_1(m-1)$ and $H = 1$. The resonance regions are labelled U_1 and U_2. The resonance region U_1 and the stable region S_1 are present for the range $H < 1$, while the resonance region U_2 and the stable region S_2 appear in the area characterized by $H > 1$. The two unstable regions bound a stable zone that occurs at $H = 1$ and is labelled S_0. It can be seen that the surface current J_f^2 is more strongly stabilizing for $H < 1$ than for $H > 1$. The strongest

https://doi.org/10.1017/S0022377801001003 Published online by Cambridge University Press

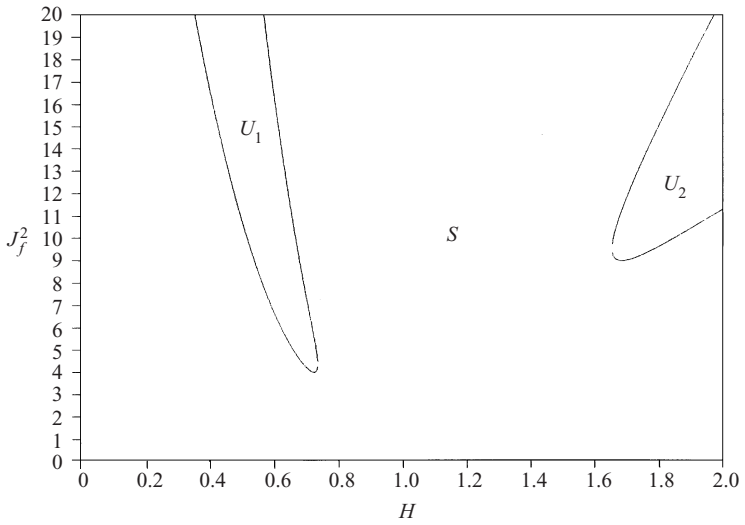

Figure 11. As in Fig. 7 but with the values of the viscosity parameters η_1 and η_2 interchanged, so that $\eta_2 > \eta_1$.

stabilizing effect occurs at $H = 1$. It is clear from this calculation that the surface currents will disappear on the interface at $H = 1$. In addition, the azimuthal magnetic field plays a stabilizing role, in agreement with case A. This stabilizing role of the magnetic field increases as J_f^2 is increased. However, a dual role of the influence of the surface current density J_f^2 is observed in this calculation.

In Fig. 8 we show a similar diagram to that in Fig. 7, but with the applied frequency $\tilde{\omega}$ changed to 30 Hz. The resonance point that occurs at $H = 1$ is not affected by the change in $\tilde{\omega}$. The increase in $\tilde{\omega}$ affects only the resonance regions. It is apparent from a comparison of Figs 7 and 8 that as $\tilde{\omega}$ is increased, the stable regions S_1 and S_2 that lie outside the resonance regions become larger, while the stable zone S_0 that lies between the unstable regions U_1 and U_2 becomes smaller. In contrast, the widths of the unstable regions decrease. The same behaviour is observed on slightly increasing the fluid column radius R to 2 cm as shown in Fig. 9. This clearly illustrates the effect of increases both in the frequency $\tilde{\omega}$ and in the fluid radius R. This phenomenon was not observed in case A.

In Fig. 10, we show a similar graph to that in Fig. 7, but with the azimuthal wavenumber m changed to 3. Owing to the increase in m, the unstable regions U_1 and U_2 leave the H axis, producing a damping effect. The three stable regions S_0, S_1 and S_2 become connected. In contrast, the width of the unstable region U_1 increases while the width of the unstable region U_2 decreases. The region U_1 leaves the H axis more rapidly than the region U_2 does. The stabilizing role of an increase in the azimuthal wavenumber m was also observed in case A, in the presence of the damping parameter.

In Fig. 11, we show a similar stability diagram to that in Fig. 7, except that the values of the viscosity parameters η_1 and η_2 are interchanged so that now $\eta_2 > \eta_1$. Here the damping role of viscosity is clearer than in the case of $\eta_1 > \eta_2$. The role of damping in the region U_2 is more significant than in the region

https://doi.org/10.1017/S0022377801001003 Published online by Cambridge University Press

U_1. The three stable regions S_0, S_1 and S_2 become connected and increase in size as the unstable zones leave the H axis. A comparison between Figs 7 and 11 shows that the surface current density plays a more strongly stabilizing role when the viscosity of the outer fluid is greater than that of the inner one.

6.2. Stability configuration for a rotating fluid column

When the angular velocity Ω is non-zero, we must study the full Mathieu equation (6.4). In what follows, we shall distinguish between two cases. The first case is that of a static magnetic field. The second is concerned with the contribution of $\tilde{\omega}$ to the stability criteria.

In dealing with a static magnetic field, the field frequency $\tilde{\omega}$ is put equal to zero in (6.4). Hence the solution of the resulting characteristic equation has an exponential form $\exp(\tilde{\sigma}t)$. The disturbance parameter $\tilde{\sigma}$ satisfies the following dispersion relation:

$$\tilde{\sigma}^2+2(a_1+ib_1)\,\tilde{\sigma}+(a_2+2ib_2+qJ_f^2)=0. \tag{6.16}$$

Zahreddine and Elshehawey (1988) established necessary and sufficient conditions for the stability of (6.16):

$$a_1>0, \qquad a_1^2(a_2+qJ_f^2)+2a_1b_1b_2-b_2^2>0. \tag{6.17}$$

In terms of the surface current density J_f, the above stability conditions are

$$\begin{aligned} J_f^2>\frac{R^2(H-1)^2}{m(\mu_1H^2+\mu_2)\,[H(m+1)-\eta(m-1)]^2}\Bigg(&m(\rho_1+\rho_2)\,[H\Omega_2(m+1)-\eta\Omega_1(m-1)]^2\\ &-2[H(m+1)-\eta(m-1)]\,[H\Omega_2(m+1)-\eta\Omega_1(m-1)]\\ &\times[\rho_2\,\Omega_2(m+1)+\rho_1\,\Omega_1(m-1)]-[H(m+1)-\eta(m-1)]^2\\ &\times\left\{\frac{(m^2-1)\,T}{R^3}-[\rho_2\,\Omega_2^2(m+1)+\rho_1\,\Omega_1^2(m-1)]\right\}\Bigg), \end{aligned} \tag{6.18}$$

provided that $H>H_c$. In the limiting case as $\Omega_1=\Omega_2=\Omega$, the above stability condition reduces to

$$J_f^2>J_0^*=\frac{R^2(H-1)^2}{m(\mu_1H^2+\mu_2)}\left[(\rho_1-\rho_2)\,\Omega^2-\frac{(m^2-1)\,T}{R^3}\right]. \tag{6.19}$$

Inspection the above stability condition shows that the angular velocity Ω plays a destabilizing role, and an increase in Ω increases the size of the unstable region bounded by the curve J_0^*, in the case of $\rho_1>\rho_2$. In the case of $\rho_2>\rho_1$, the angular velocity Ω has an effect on the stability.

Another dramatic aspect of the stability behaviour in the presence of the frequency $\tilde{\omega}$ will now be presented. We shall deal with the periodic solutions of the Mathieu equation (6.4). For periodic solutions, a stability analysis can be performed using the marginal state treatment. Marginal stability holds trivially in the inviscid case. To obtain the marginal state for rotating viscous flow, two conditions must be satisfied: a necessary condition

$$\frac{d^2\gamma}{dt^2}+2ib_1\frac{d\gamma}{dt}+(a_2+qJ_f^2\cos^2\tilde{\omega}t)\,\gamma=0, \tag{6.20}$$

https://doi.org/10.1017/S0022377801001003 Published online by Cambridge University Press

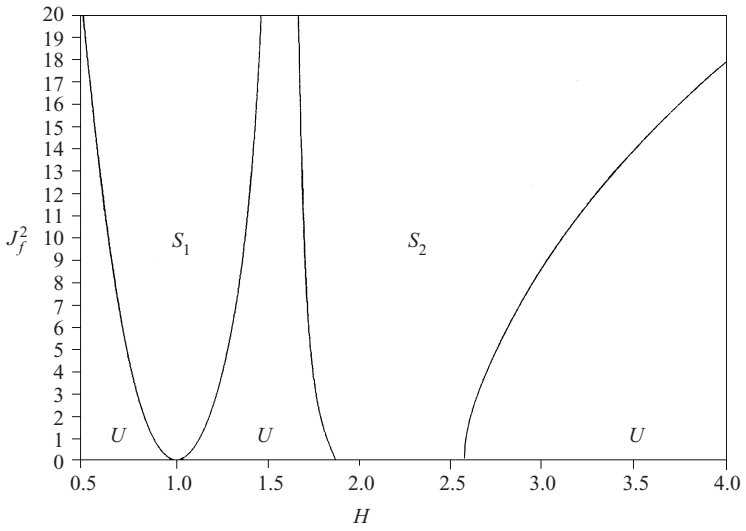

Figure 12. The graph illustrates the stability condition (6.24) for a system of fluid radius $R = 0.5$ cm, field frequency $\tilde{\omega} = 30$ Hz, stratified viscosity $\eta = 5$, azimuthal wavenumber $m = 2$ and angular velocities $\Omega_1 = 10\ \mathrm{s}^{-1}$ and $\Omega_2 = 8\ \mathrm{s}^{-1}$. The fluid densities and permeabilities are as in Fig. 7.

and a sufficient condition

$$a_1 \frac{d\gamma}{dt} + ib_2 \gamma = 0. \tag{6.21}$$

It is worthwhile observing that the equation governing the marginal state can be formulated by combining the necessary condition (6.20) with the sufficient condition (6.21) into a single condition.

To obtain the combination between the necessary condition and the sufficient condition, we need to rewrite (6.20) using (6.21) in order to introduce an undamped Mathieu equation. Clearly, a singularity occurs owing to the vanishing of the coefficient a_1. There is a singular case similar to what occurs in case A when the stratified magnetic intensity $H = 1$ (i.e. in the absence of surface currents). The condition $a_1 = 0$ means that this singularity arises at a critical value of the stratified magnetic intensity H_c given by (6.11).

If the special value H_c is excluded, the undamped Mathieu equation can be formulated from (6.20) and (6.21) in the form

$$\frac{d^2\gamma}{dt^2} + (\Delta + qJ_f^2 \cos^2 \tilde{\omega} t)\, \gamma = 0, \tag{6.22}$$

where

$$\Delta = \frac{m}{(\rho_1 + \rho_2)} \left\{ \frac{(m^2 - 1)\, T}{R^3} - [\rho_2 \Omega_2^2 (m+1) + \rho_1 \Omega_1^2 (m-1)] \right.$$

$$\left. + \frac{2[\rho_2 \Omega_2 (m+1) + \rho_1 \Omega_1 (m-1)]\, [H\Omega_2 (m+1) - \eta \Omega_1 (m-1)]}{H(m+1) - \eta(m-1)} \right\}. \tag{6.23}$$

https://doi.org/10.1017/S0022377801001003 Published online by Cambridge University Press

In the case of non-vanishing field frequency $\tilde{\omega}$, stability occurs when the following inequality is satisfied:

$$q^2 J_f^4 + 16(\tilde{\omega}^2 - \Delta)\, q J_f^2 + 32\Delta(\tilde{\omega}^2 - \Delta) > 0, \tag{6.24}$$

namely

$$(J_f^2 - J_1^{**})\,(J_f^2 - J_2^{**}) > 0, \tag{6.25}$$

where

$$J_{1,2}^{**} = \frac{8}{q}[-(\tilde{\omega}^2 - \Delta) \pm \sqrt{(\tilde{\omega}^2 - \Delta)\,(\tilde{\omega}^2 - \tfrac{3}{2}\Delta)}]. \tag{6.26}$$

The transition curves J_1^{**} and J_2^{**} should start from the point $H = 1$ and from the point satisfying $\tilde{\omega}^2 = \Delta$, which represents the resonance point. There exists another starting point satisfying $\Delta = 0$. Therefore, in the (J_f^2, H) plane, the transition curves will intersect the H axis at three points, given by $H = 1$ and $H = \lambda_j\, \eta(m-1)/(m+1)$, where $\lambda_j \neq 1$ and have the forms

$$\begin{aligned}\lambda_1 = &\left\{\frac{m(m^2-1)\,T}{R^3} - m[\rho_2\,\Omega_2^2(m+1) - \rho_1\,\Omega_1^2(m-1)] + 2m\rho_2\,\Omega_1\,\Omega_2(m+1)\right.\\ &\left.-\tilde{\omega}^2(\rho_1+\rho_2)\right\}\left\{\frac{m(m^2-1)\,T}{R^3} + m[\rho_2\,\Omega_2^2(m+1)\right.\\ &\left.-\rho_1\,\Omega_1^2(m-1)] + 2m\rho_1\,\Omega_1\,\Omega_2(m-1) - \tilde{\omega}^2(\rho_1+\rho_2)\right\}^{-1}\end{aligned} \tag{6.27}$$

$$\begin{aligned}\lambda_2 = &\left\{\frac{(m^2-1)\,T}{R^3} - [\rho_2\,\Omega_2^2(m+1) - \rho_1\,\Omega_1^2(m-1)] + 2\rho_2\,\Omega_1\,\Omega_2(m+1)\right\}\\ &\times\left\{\frac{(m^2-1)\,T}{R^3} + [\rho_2\,\Omega_2^2(m+1) - \rho_1\,\Omega_1^2(m-1)] + 2\rho_1\,\Omega_1\,\Omega_2(m-1)\right\}^{-1}.\end{aligned} \tag{6.28}$$

At $H = \eta(m-1)/(m+1)$, the transition curves will tend to infinity, giving a singular case. In order to allow a description of stability in the critical case H_c, we may rewrite the Mathieu equation (6.4) for the special value H_c. It is clear that the singularity can be relaxed when $\Omega_1 = \Omega_2 = \Omega \geqslant 0$. The coefficients Δ and q then reduce to

$$\Delta_0 = \frac{m}{\rho_1+\rho_2}\left\{\frac{(m^2-1)\,T}{R^3} + \Omega^2[\rho_2(m+1) + \rho_1(m-1)]\right\}, \tag{6.29}$$

$$q_0 = \frac{m^2[\mu_2(m+1)^2 + \mu_1\,\eta^2(m-1)^2]}{R^2(\rho_1+\rho_2)\,[(m+1) - \eta(m-1)]^2}. \tag{6.30}$$

It is clear that the assumption that $H \neq 1$ leads to $\eta \neq (m+1)/(m-1)$. The situation where $H = 1$ has been investigated in case A. Note that the presence of the surface current density J_f leads to the appearance of viscosity contributions, as shown in (6.30), rather than the similar situation in case A.

6.3. Numerical estimation and conclusions

The stability condition (6.24) has been calculated for a system with fluid radius $R = 0.5$ cm, field frequency $\tilde{\omega} = 30$ Hz, stratified viscosity $\eta = 5$, azimuthal

https://doi.org/10.1017/S0022377801001003 Published online by Cambridge University Press

wavenumber $m = 2$, and angular velocities $\Omega_1 = 10\ \mathrm{s}^{-1}$ and $\Omega_2 = 8\ \mathrm{s}^{-1}$. The fluid densities and permeabilities were as in Fig. 7. The results of calculation are displayed in Fig. 12. The stability diagram is given by a plot of the transition curves according to (6.26). The surface current density J_f^2 is plotted as a function of the stratified magnetic field. In this stability diagram, two stable regions S_1 and S_2 lie between three unstable (U) regions.

The first stable zone S_1 starts from the point $H = 1$. At the exact value $H = 1$, the azimuthal stratified field plays a stabilizing role in the absence of J_f^2. A destabilizing influence of the field appears in the neighbourhood of $H = 1$. This stabilizing influence decreases as J_f^2 increases. This shows the stabilizing influence of the presence of J_f^2 in the neighbourhood of $H = 1$. It can be recognized that this stable zone corresponds to the stable zone S_0 appearing in Figs 7–9 in the absence of the angular velocity Ω_j. The two stable regions S_1 and S_2 that appear in these figures have disappeared in Fig. 12 owing to the presence of Ω_j, which shows the destabilizing influence of Ω_j.

The second stable region S_2 in Fig. 12 appears, in the absence of J_f^2, at the values of H satisfying the following inequality:

$$\frac{\lambda_1\,\eta(m-1)}{m+1} > H > \frac{\lambda_2\,\eta(m-1)}{m+1}, \tag{6.31}$$

where the right-hand side corresponds to the case $\Delta = 0$ while the left-hand side corresponds to $\tilde{\omega}^2 = \Delta$. The calculation shows that this stable region occurs for $2.577662 > H > 1.867992$. An increase in J_f^2 leads to an increase in the size of this stable region, so that the stratified magnetic field is more strongly stabilizing in the presence of J_f^2. In the absence of J_f^2, the stratified field plays a destabilizing role for $H > \lambda_1\,\eta(m-1)/(m+1)$. The presence of surface currents has constrained this destabilizing role. In contrast with the stable region S_1, the stable region S_2 is dependent on the stratified viscosity η. An increase in the viscosity parameter increases the size of this region and shifts it in the direction of increasing H.

Inspection of the graph in Fig. 12 shows that there is a singularity for the transition curves. A major instability arises when $H = H_c$, which lies between the two stable regions S_1 and S_2. In this graph, the critical value of the stratified magnetic field is $H_c = 1.66667$. The occurrence of this singularity is dependent on the stratified viscosity η and the azimuthal wavenumber m, while it is independent of both the angular velocity Ω_j and the field frequency $\tilde{\omega}$. Very much larger values of the surface currents are required to suppress this unstable case.

The stability behaviour at the exact critical value of the stratified magnetic field is amplified in Fig. 13. The transition curves (6.26) are calculated using the parameters Δ_0 and q_0 as defined by (6.29) and (6.30) respectively. The stability diagram shows the variation of η versus J_f^2. The results of increasing m, Ω and $\tilde{\omega}$ on the stability criteria are shown respectively in Figs 13(a), (b) and (c). The system has fluid densities ρ_1 and ρ_2 and permeabilities μ_1 and μ_2 as in Fig. 12.

In Fig. 13(a), three different values of m (2, 3 and 5) are considered for fixed $\tilde{\omega} = 40$ Hz and $\Omega = 1\ \mathrm{s}^{-1}$. It is found that the maximum stability occurs when $m = 2$ at $\eta = 3$, which corresponds to the value of $H = 1$. This is in agreement with the fact that stability occurs for $H = 1$. As m is increased to 3, a very large decrease occurs in the size of the stable zone, with a shift of the point

https://doi.org/10.1017/S0022377801001003 Published online by Cambridge University Press

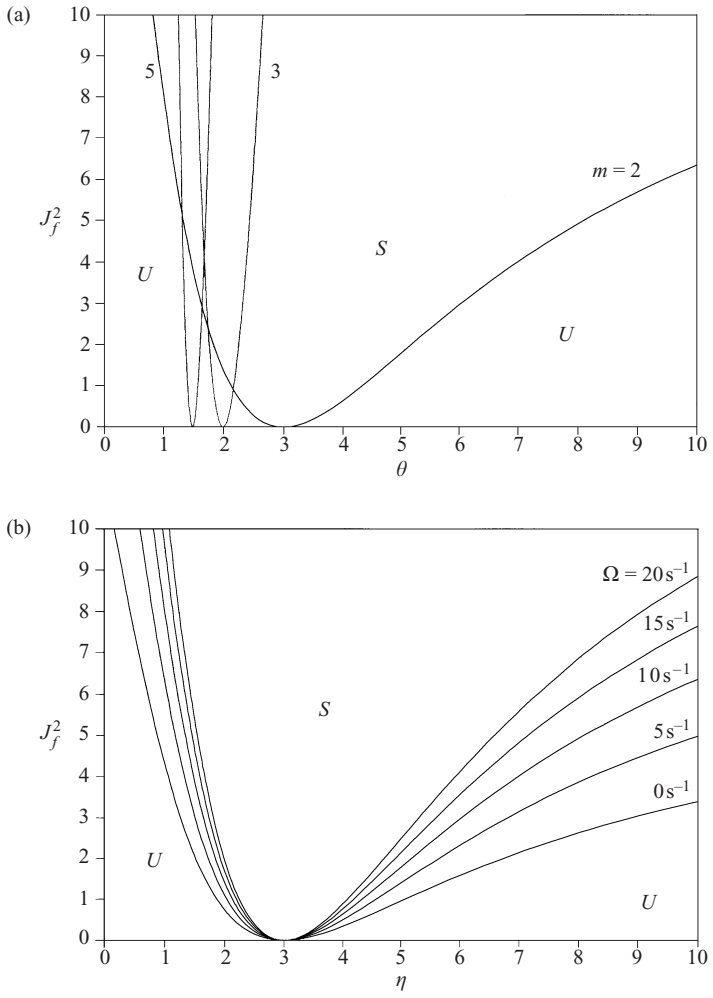

Figure 13. For caption see facing page.

representing the maximum stability to $\eta = 2$. When m is increased to 5, a very narrow stable zone is observed, and the maximum stability is at $\eta = 1.5$. However, this graph shows that an increase in the azimuthal wavenumber m, in the presence of both J_f^2 and Ω, plays a destabilizing role. The same behaviour was observed before in case A (see Fig. 2). The opposite role is observed for increasing m in the absence of Ω (see Fig. 10).

In Fig. 13(b), we show the plots in the (J_f^2, η) plane for different values of the angular velocity Ω (0, 5, 10, 15 and 20 s^{-1}), with $m = 2$ held fixed, while the other parameters are as in Fig. 13(a). It is clear from the graph that the width of the stable zone is affected by an increase of Ω, while the value of η corresponding to $H = 1$ is not affected by the variation of Ω. It is found that the size of the stable zone decreases as Ω is increased. This shows that Ω plays a destabilizing influence on the stability, which counteracts the stabilizing influence of J_f^2.

https://doi.org/10.1017/S0022377801001003 Published online by Cambridge University Press

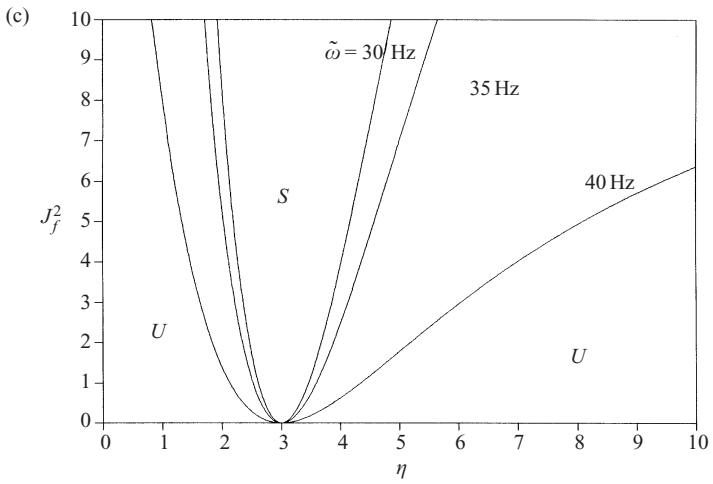

Figure 13. (a) A similar stability diagram to Fig. 12, for the variation of η versus J_f^2. The transition curves (6.26) are calculated using the parameters Δ_0 and q_0 as defined by (6.29) and (6.30) respectively. Three different values of m are considered, with fixed $\tilde{\omega} = 40$ Hz and $\Omega = 1$ s^{-1}. (b) As in (a), but for different values of the angular velocity Ω, with fixed $m = 2$. (c) As in (a), but for three different values of the field frequency $\tilde{\omega}$, with fixed $m = 2$ and $\Omega = 1$ s^{-1}.

In Fig. 13(c), we repeat the plot of Fig. 13(a) for three different values of the field frequency $\tilde{\omega}$ (30 Hz, 35 Hz and 40 Hz), with fixed $m = 2$ and $\Omega = 1$ s^{-1}. It can be seen that the stable zone that lies at $\eta = 3$ increases in width as $\tilde{\omega}$ is increased. The same behaviour was observed before in case A, where $\tilde{\omega}$ acts against the angular velocity.

Acknowledgement

The author gratefully acknowledges stimulating discussions with Professor Abou El Magd A. Mohamed.

References

Alterman, Z. 1961 *Phys. Fluids* **4**, 955.

Bauer, H. F. 1983 *Forsch. Ing.-Wes.* **49**, 117.

Bauer, H. F. 1984 *Z. angew. Math. Mech.*

Bauer, H. F. 1989 *Flugwiss. Weltraumforsch.* **13**, 248.

Chandrasekhar, S. 1961 *Hydrodynamic and Hydromagnetic Stability*. Oxford University Press.

Donnelly, R. J. 1969 *Proc. R. Soc. Lond.* **A312**, 130.

El-Dib, Y. O. 1996 *Fluid Dyn. Res.* **18**, 17.

El-Dib, Y. O. 1997 *J. Phys.* **A30**, 3585.

El-Dib, Y. O. and Moatimid, G. M. 1994 *Physica* **A205**, 511.

Gillis, J. and Kaufman, B. 1961 *Q. Appl. Maths* **19**, 301.

Grimshaw, R. 1990 *Nonlinear Ordinary Differential Equations*. Blackwell, Oxford.

Gupta, A. S. 1964 *Proc. R. Soc. Lond.* **A278**, 214.

Hocking, L. M. and Michael, D. H. 1959 *Mathematika* **6**, 25.

McLachlan, N. W. 1964 *Theory and Application of Mathieu Functions*. Dover, New York.

Melcher, J. M. 1963 *Field-Coupled Surface Waves*. MIT Press, Cambridge, MA.
Moatimid, G. M. and El-Dib, Y. O. 1994 *Int. J. Eng. Sci.* **32**, 1183.
Mohamed, A. A. and Nayyar, N. K. 1970 *J. Phys.* **A3**, 296.
Mohamed, A. A., El-Sakka, A. G. and Sultan, G. M. 1985 *Physica Scripta* **31**, 193.
Nayfeh, A. H. and Mook, D. T. 1979 *Nonlinear Oscillations*. Wiley, New York.
Nayyar, N. K. and Terhan, S. K. 1963 *Phys. Fluids* **6**, 1587.
Rayleigh, Lord 1878 *Proc. Lond. Math. Soc.* **10**, 4.
Schwabe, D. 1988 *Crystals* **11**, 75.
Srivistava, K. M. and Kushwaha, R. S. 1967 *Nuovo Cim.* **B51**, 535.
Terhan, S. K., Malik, S. K. and Dikshit, M. S. 1965 *Phys. Fluids* **8**, 1461.
Verma, P. and Verma, Y. K. 1965 *J. Fluid Mech.* **22**, 33.
Wilson, S. K. 1992 *Q. J. Mech. Appl. Maths* **45**, 363.
Zahreddine, Z. and Elshehawey, E. F. 1988 *Indian J. Pure Appl. Maths* **19**, 963.